LIDAR mapping of ozone-episode dynamics in Paris and intercomparaison with spot analysers

Alexandre Thomasson, Sylvain Geffroy, Emeric Frejafon, Derk Weidauer, R. Fabian, Yves Godet, Michel Nomine, Tamara Menard, Pierre Rairoux, D. Moeller, et al.

LIDAR MAPPING OF OZONE EPISODE DYNAMICS IN PARIS AND INTERCOMPARISON WITH SPOT ANALYZERS

A. Thomasson [1+], S. Geffroy [1], E. Frejafon [2], D. Weidauer [4], R. Fabian [3], Y. Godet[2], M. Nominé [2], T. Ménard [2], P. Rairoux [1], D. Moeller [3], and J.P. Wolf [1, *].

(1) LASIM, UMR CNRS 5579, Bât. A. Kastler, Université Claude Bernard Lyon 1, 43 Bd du 11 Novembre 1918, 69622 Villeurbanne cedex, France

(2) INERIS, Parc technologique ALATA, BP 2, 60550 Verneuil-en-Halatte, France

(3) Inst. fuer Luftchemie, BTU-Cottbus, Vollmer Strasse 13, 12489 Berlin, Germany

(4) Elight Laser Systems GmbH, Warthestrasse 21, 14513 Teltow/Berlin, Germany

(+) present address : COPARLY, rue des Frères Lumières, 69120 Vaulx-en-Velin, France

(*) Corresponding author: (Fax: +33 4 72 43 15 07, e-mail: wolf@lasim.univ-lyon1.fr)

Abstract.

Continuous mapping of an ozone episode in Paris in June 1999 has been performed using a Lidar-DIAL System. The 2D ozone concentration vertical maps recorded over 33 hours at the Champ de Mars are compiled in a video clip that gives access to local photochemical dynamics with unprecedented precision. The Lidar data are compared over the whole period with point monitors located at 0, 50, and 300 m altitudes on the Eiffel Tower. Very good agreement is found when spatial resolution, acquisition time, and required concentration accuracy are optimized. Sensitivity on these parameters for successful intercomparison in urban areas is discussed.

PACS : 42.68.W; 92.60.S; 07.07.V; 82.33.T

I. Introduction

Differential Absorption Lidar (DIAL) has, in the recent years, been widely used to characterize urban and industrial pollution. Its unique feature of providing 2D- and 3D-maps of pollutant concentrations at high sensitivity (in the parts per billion range) and over large distances (several km) has appeared as extremely valuable to quantify the impact of spot emitters, monitor urban pollution [16], or evaluate predictive numerical models [1].

A key issue, however, to further use the Lidar technique for enforcement purposes in environmental protection agencies is the evaluation of Lidar systems within the framework of the present standards. This evaluation process can be achieved with two different types of experiments: (1) Evaluation using reference gases within procedures in agreement with national standards [12, 17, 18] and (2) Intercomparison with calibrated gas analyzers. In this latter case, the main difficulty is to find a site where the DIAL measurement (representing an average over some tens or hundreds of meters) can successfully be compared to values provided by spot monitors. This requires specific conditions where concentration gradients are small compared to the detection limits of the devices. In case of ozone, former intercomparison campaigns have therefore been performed in the countryside where no local nitrogen oxide s sources were present [4]. Recently a campaign has been performed in Berlin (OLAK) in order to intercompare Lidar systems and airborne ozone analyzers in urban conditions [5]. Comparison with airborne measurements is difficult because the measured air volumes by the Lidars and the balloon- or aircraft-borne analyzers are never exactly the same.

We present here a continuous mapping of ozone in a large urban area, synchronously compared to spot measurements at different altitudes, over a 33 hour ozone episode. This continuous mapping, which has been displayed as a video clip [ref electronic journal version], depicts the whole ozone episode dynamics. Compared to former studies, in Athens [6,13, 15]

or Seville [7, 8], the obtained succession of ozone 2D-maps (vertical profiles) provide significantly more information about local gradients and mass transfers.

Continuous intercomparison at three altitudes (up to 300 meters) moreover allowed to verify whether this evaluation procedure is suitable in urban areas and to find the origin of potential discrepancies between DIAL measurements and spot analyzers.

2. Experiment

In 1999, INERIS [1], which is in charge in France of calibrating and evaluating optical systems such as DOAS and Lidar, organized a large Lidar ozone measurement campaign in Paris from July 12 to 20. This campaign was performed under the French Ministry of Environment's coordination[2], in collaboration with AIRPARIF (Air Quality Network of Paris and the Region Ile de France). The main purpose was the evaluation of a ~~n~~ ozone Lidar working in actual urban conditions.

A key feature to successfully achieve this study was to use a reliable, easy to operate DIAL system. The chosen system is a 'Lidar 510 M' model, manufactured by Elight Laser Systems. This mobile (van-integrated) all-solid-state DIAL system has been extensively described elsewhere [2]. Briefly, it is based on a flashlamp-pumped Ti:Sapphire laser, with a dual wavelength oscillator (for both reference λ_{off} and probe λ_{on} wavelengths), which provides after frequency doubling and tripling some mJ between 250 nm and 290 nm. Both wavelengths position and linewidths are controlled using an optogalvanic reference cell

[1] INERIS: Institut National de l'Environnement Industriel et des Risques
[2] MATE: Ministère de l'Aménagement du Territoire et de l'Environnement

(Galvatron). The laser beam is 10X expanded to emit radiation well below limits of eye safety requirements (according to VDI-DIN 0837).

The laser beam is sent into the atmosphere with a dual scanning periscope that also directs the backscattered light back to the 400 mm/f3 telescope. The signal is detected by a photomultiplier, through a motorised monochromator, in order to automatically select the proper detected wavelength range. The signal is digitised by a 12 bits 20 MHz transient recorder, allowing an ultimate spatial resolution of 7.5 m (for some emission measurements faster 8 bits A/D converters are used). The data are handled by a PC-microcomputer that also controls every system parameters: wavelength setting and calibration, receiver parameters (PMT-high voltage, preamplifier gain, spectrometer settings,..) and periscope steering in azimuth and elevation. The software is Windows-based, and includes a sophisticated inversion algorithm optimizing the S/N ratio, and modules for automatic operation, and on-line evaluation of the data.

This DIAL provides concentration maps of O_3, SO_2, NO_2, Benzene and Toluene. For ozone, the standard wavelength couple is λ_{off} = 286.3 nm and λ_{on} = 282.4 nm. The manufacturer specifies a detection limit of 2 $\mu g/m^3$ (for 1 km integration length, 15 min. integration time) and a maximum measurement distance of 2500 m, according to the VDI-DIN 3210 standard [12]. Evaluation at INERIS using reference gases [3] yielded slightly higher detection limits (4-6 $\mu g/m^3$) but longer maximum distance (3500 m).

The DIAL system was located at the Champ de Mars facing the Eiffel Tower. This site provided free optical path over 1.4 km, without major traffic roads, limiting local nitrogen oxides gradients. Reference ozone analyzers from AIRPARIF were located at three different levels at the Eiffel Tower (ground, 50 m. and 300 m.). Intercomparison between Lidar and

spot monitors data could be obtained at these three altitudes over 33 continuous hours, during an ozone smog episode. The reference spot monitors form AIRPARIF (from "Thermo Electron" and "Environment S.A.") are specified with a detection limit below 5 $\mu g/m^3$. They are calibrated every 3 months using a NIST standard transfer, and maintenance is carried out twice a month. Sampling uses PFA-Teflon pipes of a few meter length. This equipment is completed by NOx and SO_2 analyzers, temperature sensors, and, at 300m high, wind direction/velocity measurements (sonic anemometers).

3. Results

2D-maps of ozone concentrations have been recorded by accumulating 1000 shots in each measurement direction (500 on λ_{on} and 500 on λ_{off} representing 1 minute) over 33 hours (Sat. 07/17 – Mon. 07/19). Six principal measurement directions have been chosen, as presented in figure 1, three of which corresponding to altitudes at the Eiffel Tower (900 m from the system) where the reference analyzers were set. Spatial interpolation using a gaussian filter over the 6 radial profiles yields a vertical 2D-map of the ozone concentration at a time interval of 15 minutes. The 2D-maps have been compiled in a sequential dynamic representation [see electronic version], which constitutes the first 'video clip' depicting the ozone smog formation processes within a large city. For the print format, we present here a series of representative snapshots sorted out from this video (Figure 2 (a)-(j)).

An important consideration for all the presented results is the Rayleigh/Mie correction applied to take into account the difference in scattering cross-sections at λ_{off} = 286.3 nm and λ_{on} = 282.4 nm. In first approximation, we only considered the effects due to Rayleigh/Mie

extinction (assuming homogenous aerosol distribution in the atmosphere). In this framework, an offset correction ΔC_{RM} is applied to all the ozone concentration values:

$$\Delta C_{RM} = \frac{MM}{\Delta\sigma_A}(\Delta\alpha_R + \Delta\alpha_M)$$

where MM is the ozone molecular mass, $\Delta\sigma_A = \sigma_A(\lambda_{on}) - \sigma_A(\lambda_{off})$ is the ozone differential absorption cross-section, $\Delta\alpha_R = \alpha_R(\lambda_{on}) - \alpha_R(\lambda_{off})$ and $\Delta\alpha_M = \alpha_M(\lambda_{on}) - \alpha_M(\lambda_{off})$ are the difference in Rayleigh and Mie extinction coefficients for the considered wavelength couple. For Rayleigh scattering (1013 mbar, 298 K) [10], this yields to a correction of -4 $\mu g/m^3$. For Mie scattering, a first order empirical correction has been used, based on the meteorological visibility range V_M [10]. In our case the visibility range of 13 km (clear atmosphere) yields a systematic correction of -10 $\mu g/m^3$. The errors induced by these constant corrections are discussed below.

The snapshots selected from the video clip, in figure 2(a)-(j), very well depict the formation dynamics of the ozone episode in Paris. On figures 2(a)-(d) (Saturday July 17, 21:00 – Sunday July 18, 08:30, local time), the maps show with unprecedented realism the destruction of ozone at lower altitudes mainly by the traffic emitted NO at night. This lower ozone concentration (around 50 $\mu g/m^3$) is confined in a layer of 120-280 m thick close to the ground. At higher altitudes (from 280 m - >1500 m), a much higher concentration (80-150 μg/m3) layer seems unperturbed by the NO emitted at ground level. This suggests that most of the traffic related NO has been consumed in the reaction converting O_3 into NO_2 within a vertical diffusion length of typ. 300 m (which corresponds to the urban layer). While depletion at low altitude exhibits a strong diurnal cycle, the ozone concentration above 300 m remains high regardless the daily hour. This behavior has been observed in other cities, and is referred to as the "tropospheric ozone storage layer" [16, 15]. Notice also that small scale

fluctuations appear within the storage layer and on the border of the storage layer and the mixing layer.

This vertical double layers structure remains over the night until 7 a.m. (local time). From 7 a.m. to 12 p.m. a very interesting vertical mixing occurs, as shown in figures 2(c)-(g). The process occurs first locally (see localized ozone bubbles at about 600 m. from the Lidar system) and then on larger scale over the whole mixing layer. A major reason for this is convection and turbulence induced by solar heating of the ground and lower atmospheric air layers. Diurnal solar radiation also photodissociates the NO_2 present at that time, the concentration of which has been enriched by the nighttime reactions between O_3 and NO. The NO_2 photolysis creates NO + O* and thus regenerates ozone in the whole afternoon until 9 p.m. This well known photocycle leading to the Leighton relationship [9], although very simple, can reasonably explain the observed behavior, since ozone generation in this case is NOx-limited [11]. For a quantitative evaluation of the processes, numerical photochemical codes including volatile organic compounds (VOCs) reactions have to be used. Comparison of such models with the maps presented here, but this is beyond the scope of the present paper.

The concentration distribution in the afternoon of July 18th is very homogenous and of very high absolute value (170-220 $\mu g/m^3$), characteristic of an ozone episode. Notice the limited Lidar measurement range, due to the very high ozone absorption. At this point, a change of the selected (λ_{off}, λ_{on}) wavelength couple towards less absorbed wavelengths (300 nm) would have been judicious. However, we decided to keep all parameters identical during the whole episode.

In the evening of July 18 (figure 2(g)-(h)) the lower atmospheric layer clears up again due to the lack of solar radiation and the presence of traffic related NO emission. The following night dynamics (figure 2(i)-(j)) is similar to the situation of the night from July 18-19.

From the successive 2D-maps, ozone vertical profiles can be computed for any horizontal location. Figure 3 shows the ozone vertical profiles at the level of the Eiffel Tower over the 33 hours. This figure very well summarizes the observations depicted above: ozone destruction at low altitude during the night, quasi homogenous storage layer above 300 m., overall ozone concentration increase due to solar radiation at daytime, mixing of both layers around 10 a.m. (local time, TU+2h) leading to homogenous high concentrations in the afternoon. However, this representation does not show the local dynamics and exchanges observed in the series of 2D-maps.

4. Intercomparison

As mentioned above, three of the measurement directions were chosen in order to analyze air volumes at the Eiffel Tower location as close as possible to the reference point sensors installed by AIRPARIF. Figure 4(a)-(c) shows the intercomparison between Lidar and spot analyzers at the 3 different altitudes (ground level, 50 m, and 300 m) with a range resolution ΔR on the Lidar profile of 200 m at the Eiffel Tower location. The experimental accuracy on the point sensors data are typically 15%, according to the users experience, while a statistical

différence

height	Δt	15min		1h	
	ΔR	200m	1km	200m	1km
20m	mean	0,46	4,07	-0,05	-0,24
	~~confidence~~	1,72	4,42	1,84	4,66
50m	mean	0,39	-4,84	1,52	-3,12
	~~confidence~~	2,47	3,31	4,04	4,46
300m	mean	-0,66	-4,81	-0,55	-5,02
	~~confidence~~	3,49	3,96	5,47	7,04

Standard deviation

Legende.

treatment of the Lidar data yields experimental standard deviation between 15 to 20 $\mu g/m^3$ depending on the measurement configuration (temporal and spatial integration). As it can be seen from these temporal profiles, the overall behavior as well as the absolute values are excellent agreement at every altitudes and over the whole period. More precisely, figure 5 presents the histogram of differences between the ozone concentrations measured by the sensors and the ones measured by Lidar: $\Delta C = C_{Sensor} - C_{Lidar}$. The mean value of ΔC (offset) is of the order of 1 $\mu g/m^3$, while the standard deviation on the difference (statistical errors) $\sigma(\Delta C)$ is only a few $\mu g/m^3$ as well. This is particularly satisfactory since the measured values spans a very broad concentration range from 20 to 180 $\mu g/m^3$. It is also interesting to observe that in stable and reasonably clear weather conditions, first order constant Rayleigh-Mie corrections are sufficient to obtain very satisfactory results. In atmospheric conditions exhibiting strong aerosol gradients this would obviously not be the case anymore.

Further intercomparison statistics have been performed for different Lidar spatial resolutions (ΔR=200 m. and ΔR=1000 m) and different "integration times" (15 minutes and 1 hour). On this latter point, it is important to notice that in a 15 minutes measurement cycle, the actual Lidar acquisition time for one reference point is only 1 minute (1000 shots averaged on each direction of the scan, see section 3). For the hourly values, four successive Lidar measurements at 15 minutes interval are averaged. The results are summarized in table 1. Best agreement is found for ΔR=200 m. Averaging over 4 measurements (hourly comparison) does not improve the statistical result, indicating that significant ozone concentration fluctuations occur on shorter timescales. An interesting feature is that spatial averaging on longer distances along the beam degrades the results as well. The reason is spatial fluctuations of the ozone concentration. Averages over longer distances are less comparable to the air volume measured by the spot monitor. This is very well illustrated by the observed negative offset

increasing with altitude on the 1 km averaged results (table 1). As shown in figure 2, ozone is destroyed at low altitude at night. Since the beams are sent at finite angles (figure 1), averaging over 1 km necessarily integrates lower ozone concentration values from low altitude leading to a negative offset compared to the concentration at the Eiffel Tower level. Spatial fluctuations of typical characteristic lengths of 50 m are also clearly observed on the video clip or the snapshots of figure 2.

5. Conclusion

Very satisfactory Lidar-sensor intercomparison can be achieved in actual urban measurement conditions results if the atmospheric spatial and temporal fluctuations are matched with the respective resolutions of the devices. In particular, a compromise has to be found between two opposite requirements: (1) spatial averaging improves the signal to noise ratio (SNR) of the Lidar data and thus the accuracy of the concentration measurements, and (2) averaging over longer paths provides mean values that are less comparable to spot measurements because of local concentration gradients. In our conditions, the optimum parameters were ΔR=200 m associated with an accuracy of 15 $\mu g/m^3$. However, these values are connected with the 1 minute time averaging. If only one measurement direction had been chosen, and intercomparison with only one spot monitor, the Lidar data could have been continuously averaged over 15 minutes, significantly improving the SNR. The accuracy and/or spatial resolution could thus have been further improved accordingly. This strategy, however, would have prevented 2D-mapping of the ozone concentration, which was the other main goal of the campaign.

Acknowledgements

The authors acknowledge Jerome Kasparian for fruitful discussions and suggestions. J.P.W. acknowledges the Institut Universitaire de France for support.

6. References

1. Beniston, M. , M. Beniston-Rebetez, H.J. Kölsch, P. Rairoux, J.P. Wolf and L. Wöste, J.Geophys.Res., **95** (D7), 9879-9894 (1990)

2. Elight Laser Systems GmbH, Elight Laser Systems, Warthestrasse 21, D-14513 Teltow/Berlin; http://www.elight.de (1999)

3. Godet Y., A. Thomasson, M. Nominé and T. Ménard, rapport INERIS (Institut National de l'Environnement Industriel et des Risques) - Loi sur l'Air – Convention 13/98, Verneuil-en-Hallate (1999)

4. Goers U.B., Optical Engineering **34**(11), 3097-3102 (1995)

5. GKSS Report 2000/24, ISSN 0344-9629, GKSS-Library, Postfach 1160, D-21494 Geesthacht (Germany) (2001)

6. Fiorani L., B. Calpini, A. Clappier, L. Jaquet, F. Müller, H. van den Bergh, E. Durieux, A. Ansmann, R. Neuber, P. Rairoux, U. Wandinger, Eds., Springer Verlag, Heidelberg, p. 367-369 (1996)

7. Frejafon, E., J. Kasparian, P. Rambaldi, B. Vezin, V. Boutou, J. Yu, M. Ulbricht, D. Weidauer, B. Kraemer, T. Leisner, P. Rairoux, L. Woeste and J.P. Wolf, Europ. Phys. Journal D **4**, 231-238 (1998)

8. De Saeger E, Report ERLAP 9, JRC, Ispra (1996)

9. Leighton P.A., Academic Press, New York (1961)

10. Measures R.M., Wiley, New York , (1984)

11. National Research Council, ISBN 0-309-04631-9, National Academy Press, Washington, 475 pp (1992)

12. VDI-DIN 4210, VDI-DIN Handbuch Reinhaltung der Luft, Band 5, Beuth Verlag Berlin (1997)

13. Weidauer, D. ,P. Rairoux, M. Ulbricht, J.P. Wolf, L. Wöste, Advances in Atmospheric Remote Sensing with Lidar, A. Ansmann, R. Neuber, P. Rairoux, 14. U. Wandinger, Eds., Springer Verlag, Heidelberg, pp. 423-426, (1996)

15. Weidauer D., H.D. Kambezidis, P. Rairoux, D. Melas, M. Ulbricht, Atmosph. Environ. **32**, 2173-2183 (1998)

16. Wolf, J. P., in: Meyers, R. A. (Ed.), Encyclopedia of Analytical Chemistry, 3. J. Wiley & Sons, New York, pp 2226-2247 (2000)

17. T. Ménard, E. Vindimian, Y. Godet, D. Weidauer, M. Ulbricht, P.Rambaldi, M. Douard, J.P.Wolf, Poll.Atmos. 10-12, 105-119 (1998)

18. Eickel, K.H. ,P. Rairoux, M. Ulbricht, D. Weidauer, K. Weber, J.P. Wolf, in Quality Assurance and Standardisation of Remote Sensing Methods, K. Weber, ed. SPIE Vol. **3106** (1997)

Figure Captions

Fig 1 : Measurement site and principal Lidar measurement directions. The 3 lowest angles are selected in order to match the location of reference ozone sensors on the Eiffel Tower.

Fig 2 : Continuous Lidar 2D-mapping of the ozone episode (snapshots form the video clip, which can be integrally seen on the electronic version of the paper).

Fig 3 : Evolution of the ozone vertical profiles, measured by Lidar, at the Eiffel Tower. location

Fig 4 : Intercomparison between reference spot analyzers and Lidar data at 3 different altitudes for 200 m of integration path at 15 min time interval (a,c).

Fig 5 : Histogram of the concentration differences ΔC between spot analyzers and Lidar.

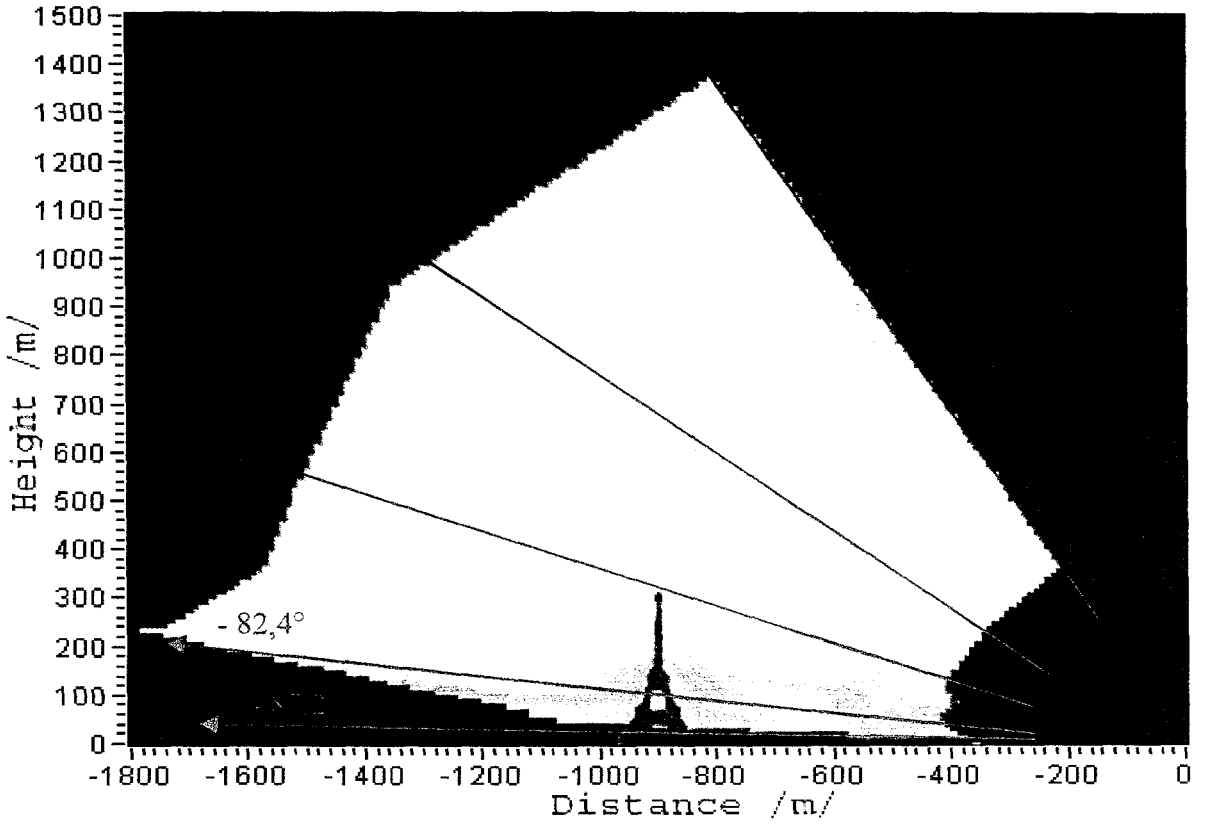
1500
1400
1300
1200
1100
1000
900
800
700
600
500
400
300
200
100
0
Height /m/
- 82,4°
-1800
-1600
-1400
-1200
-1000
-800
-600
-400
-200
0
Distance /m/

a) 17/07/1999 – 21h00

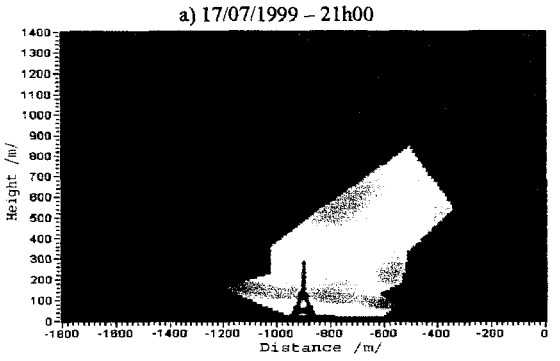

b) 18/07/1999 – 00h30

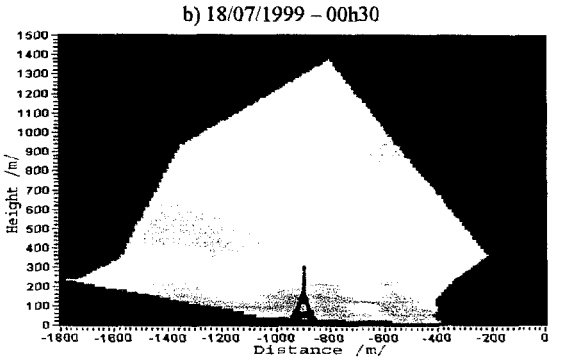

c) 18/07/1999 – 04h30

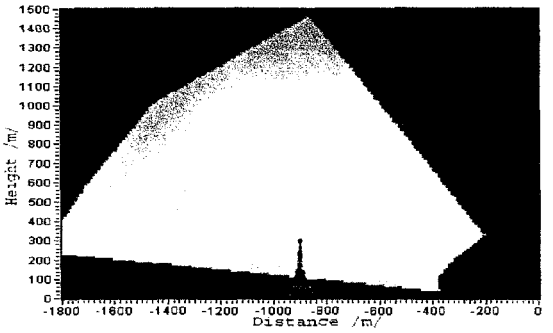

d) 18/07/1999 – 08h30

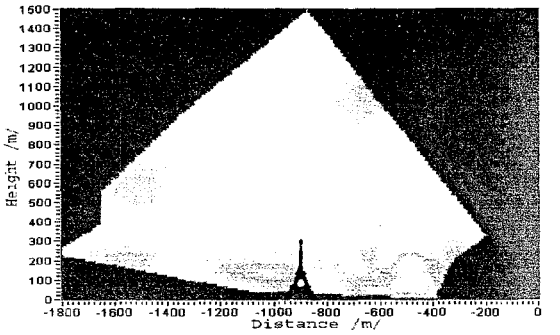

e) 18/07/1999 – 12h30

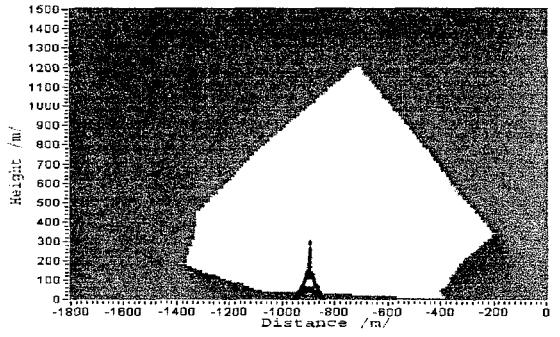

f) 18/07/1999 – 16h30

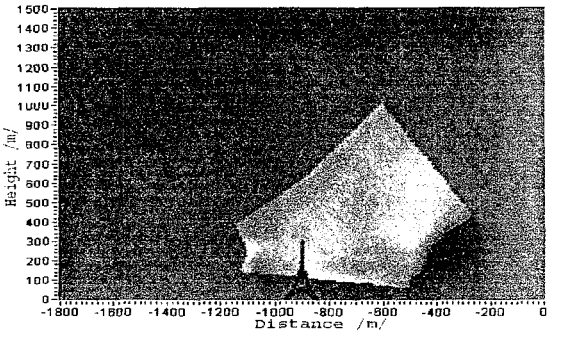

g) 18/07/1999 – 20h15

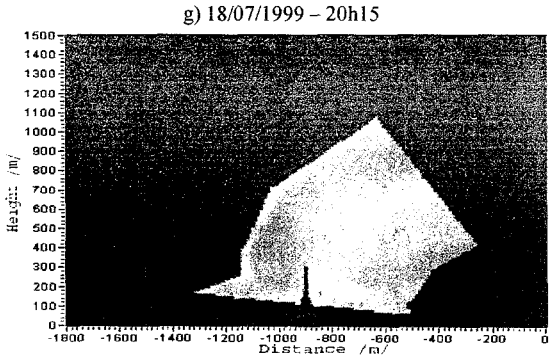

h) 18/07/1999 – 00h30

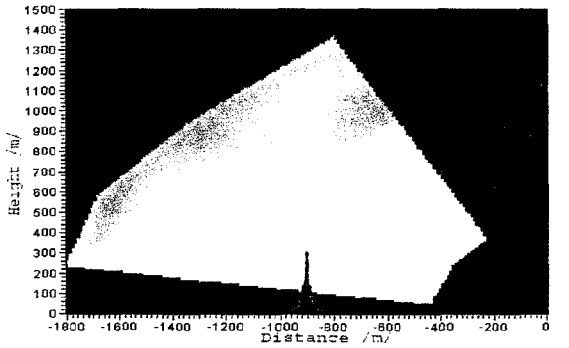

i) 19/07/1999 – 03h45

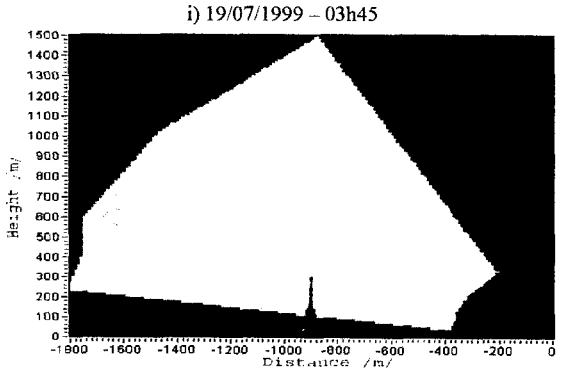

j) 19/07/1999 – 08h00

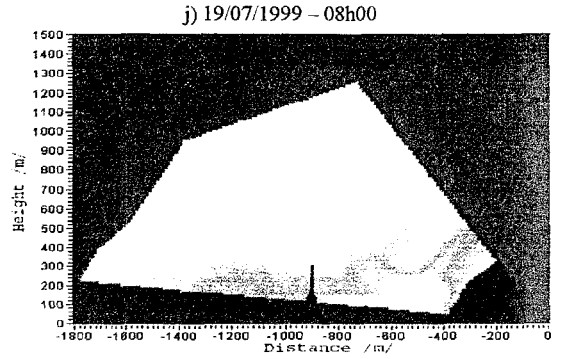

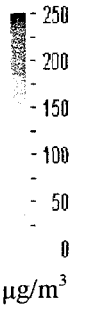

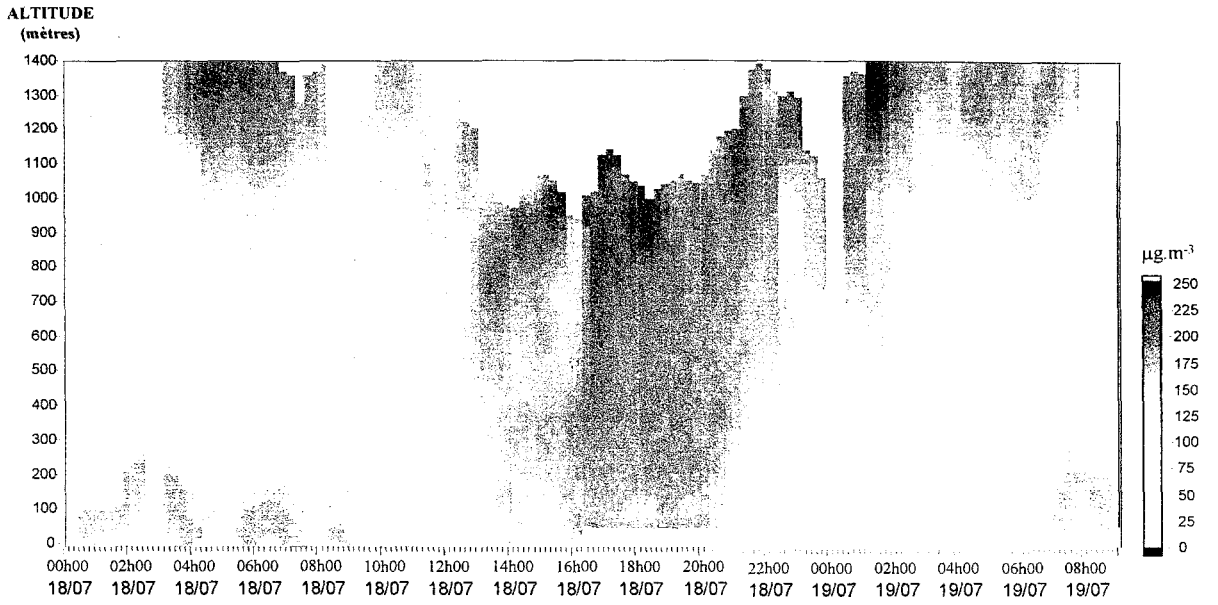
ALTITUDE
(mètres)
1400
1300
1200
1100
1000
900
800
700
600
500
400
300
200
100
0
00h00 18/07
02h00 18/07
04h00 18/07
06h00 18/07
08h00 18/07
10h00 18/07
12h00 18/07
14h00 18/07
16h00 18/07
18h00 18/07
20h00 18/07
22h00 18/07
00h00 19/07
02h00 19/07
04h00 19/07
06h00 19/07
08h00 19/07
µg.m-3
250
225
200
175
150
125
100
75
50
25
0

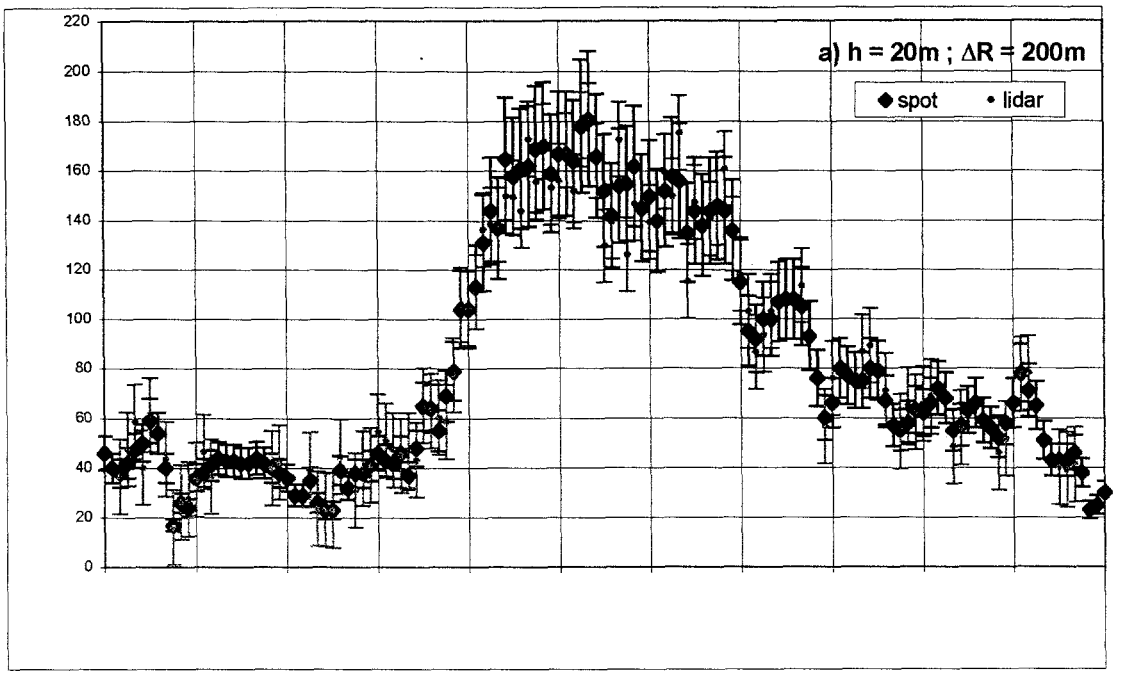
a) h = 20m ; ΔR = 200m
spot
lidar
220
200
180
160
140
120
100
80
60
40
20
0

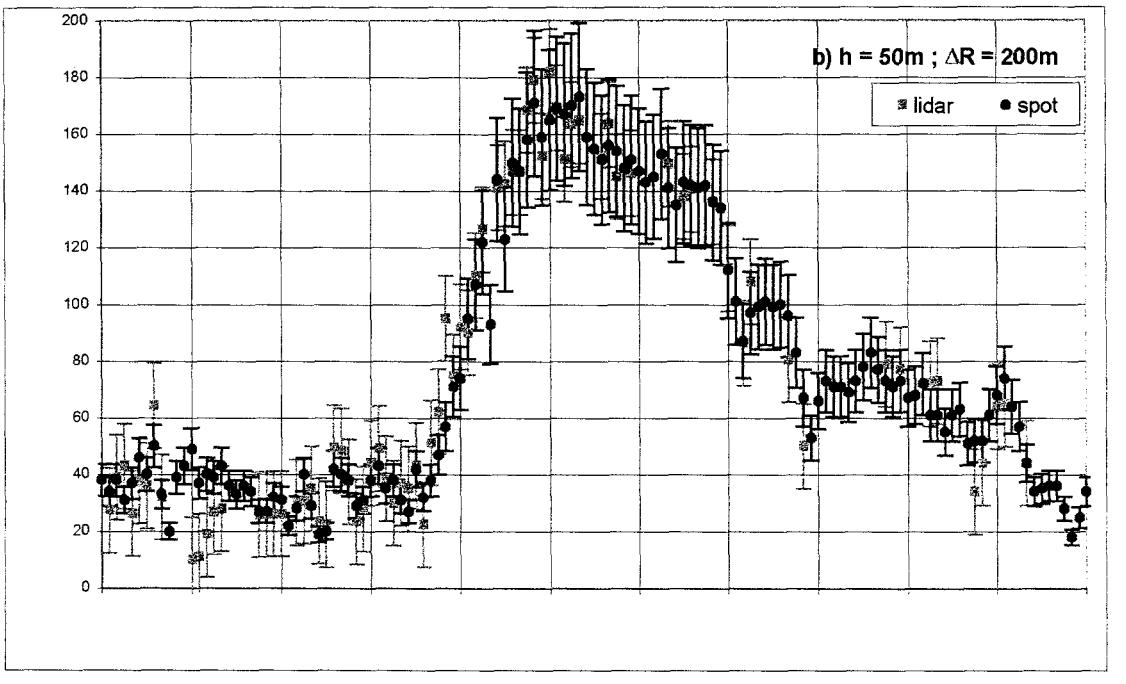
b) h = 50m ; ΔR = 200m
lidar
spot
200
180
160
140
120
100
80
60
40
20
0

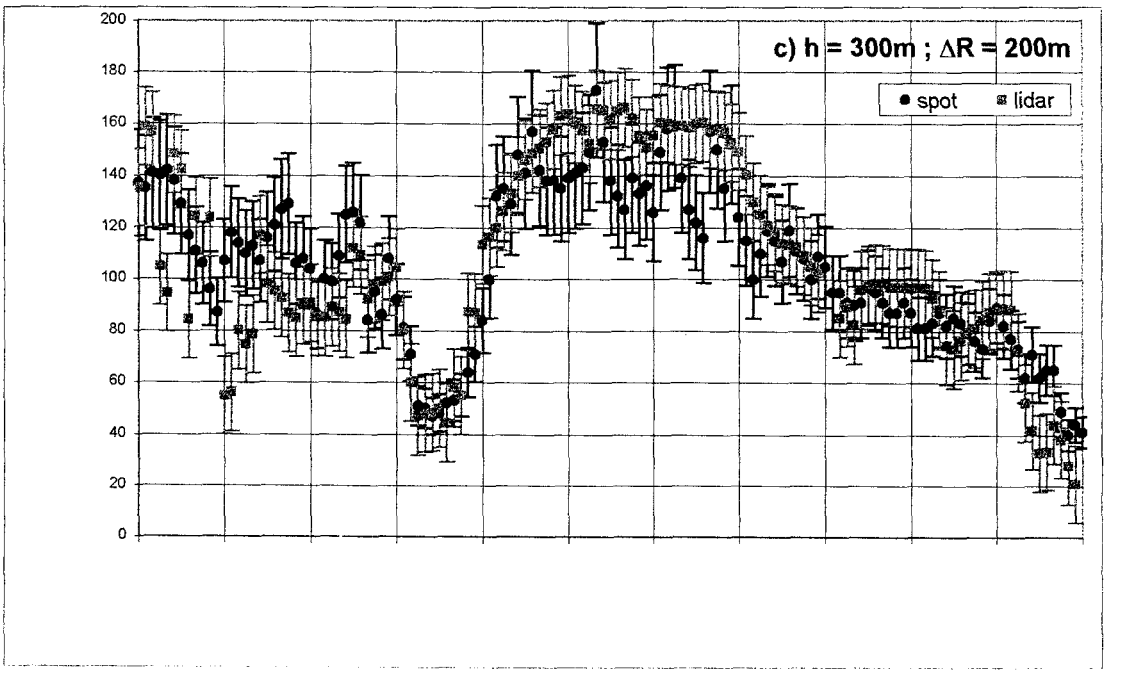
c) h = 300m ; ΔR = 200m
spot
lidar
200
180
160
140
120
100
80
60
40
20
0

h=300 m ; ΔR=200 m ; Δt=15 min